

Supporting Information

Oxidative Dehydrogenation of Propane on Silica-Supported Vanadyl Sites Promoted with Sodium Metavanadate

Manouchehr Nadjafi,[†] Agnieszka M. Kierzkowska,[†] Paula M. Abdala,[†] Rene Verel,[‡] Olga V. Safonova,[§] Alexey Fedorov,^{*†} and Christoph R. Müller^{*†}

[†] Department of Mechanical and Process Engineering, ETH Zürich, Leonhardstrasse 21, CH-8092 Zürich, Switzerland

[‡] Department of Chemistry and Applied Biosciences, ETH Zürich, Vladimir-Prelog-Weg 1-5, CH-8093 Zürich Switzerland

[§] Paul Scherrer Institute, CH-5232 Villigen, Switzerland

*E-mail: fedoroal@ethz.ch (A.F.).

*E-mail: muelchri@ethz.ch (C.R.M.).

Table of Contents

List of Figures	2
General Experimental	3
Equations	4
References.....	17

List of Figures

Figure S1. Raman spectra of the studied materials in the range 100–1450 cm ⁻¹	5
Figure S2. Raman spectra of α -NaVO ₃ /1 during in situ calcination (Linkam CCR1000 cell).	5
Figure S3. Room temperature Raman spectra of different areas of calcined α -NaVO ₃ /1 (traces a-d) after exposure to air.	6
Figure S4. DSC measurement of α -NaVO ₃ /1 calcination.....	6
Figure S5. (a) ⁵¹ V, and (b) ²³ Na MAS NMR data for as synthesized β -NaVO ₃ and α -NaVO ₃	7
Figure S6. (a) ⁵¹ V and (b) ²³ Na MAS NMR of α -NaVO ₃ /SiO ₂ (catalyst made from β -NaVO ₃ precursor).....	7
Figure S7. V K-edge XANES spectra of the reference compounds selected to show the dependence of the pre-edge peak height on the ligand geometry of vanadium.	8
Figure S8. XANES spectra of Na _{1+x} V ₃ O ₈ /SiO ₂ vs 1 (hydrated).	8
Figure S9. XANES spectra of Na _{1+x} V ₃ O ₈ /SiO ₂ (air-300) and 1 _(air-300) (dehydrated).	9
Figure S10. Raman mapping of Na _{1+x} V ₃ O ₈ /SiO ₂ (air-500).	9
Figure S11. H ₂ temperature-programmed reduction (TPR) profile of the studied catalysts.	10
Figure S12. V K-edge XANES spectra of α -NaVO ₃ /SiO ₂ (synthesized from β -NaVO ₃), β -NaVO ₃ and α -NaVO ₃	10
Figure S13. Selectivity vs. conversion plot for studied catalysts.....	11
Figure S14. ODP propene selectivity and specific activity with TOS for β - and α -NaVO ₃ /1 _(0.7)	11
Figure S15. Propene selectivity and production rate vs TOS for Na _{1+x} V ₃ O ₈ /SiO ₂	12
Figure S16. Raman spectra of α -NaVO ₃ /1 _(0.7) and β -NaVO ₃ /1 _(0.7) compared to the other materials.	12
Figure S17. Linear combination fitting (LCF) of the V K-edge XANES of β -NaVO ₃ /1 after 4h of reaction under ODP conditions.....	13
Figure S18. a) XRD and b) Raman data for as synthesized β -NaVO ₃ and α -NaVO ₃	13
Figure S19. High-angle annular dark field (HAADF) scanning transmission electron microscopy (STEM) and energy dispersive X-ray (EDX) mapping of 1.	14
Figure S20. High-angle annular dark field (HAADF) scanning transmission electron microscopy (STEM) and energy dispersive X-ray (EDX) mapping of α -NaVO ₃ /1.....	14
Figure S21. O ₂ conversions (X _{O₂}) and CO/CO ₂ molar ratios vs propane conversions (X _{C₃H₈}) for the studied catalysts.	15
Figure S22. Propene selectivity (S _{C₃H₆}) and productivity vs propane conversion (X _{C₃H₈}) at different temperatures for air treated (1 h) β -NaVO ₃ /1 catalyst.	15
Figure S23. O ₂ conversions (X _{O₂}) and CO/CO ₂ molar ratios vs propane conversions (X _{C₃H₈}) at different temperatures for β -NaVO ₃ /1.	16

General Experimental

Materials. The following materials were purchased from commercial providers and used without further purification unless mentioned otherwise: sodium hydroxide (certified AR for analysis, Fischer Scientific), vanadium (IV) oxide ($\geq 99.0\%$, Strem Chemicals), vanadium (III) oxide ($\geq 98.0\%$, Sigma-Aldrich), vanadium (V) oxide ($\geq 98\%$, Sigma-Aldrich), ammonium metavanadate ($\geq 99\%$, Acros Organics), sodium metavanadate ($\geq 99.9\%$, Sigma-Aldrich, Lot #BCBR1531V), oxalic acid dihydrate (≥ 99.0 , Fisher Scientific), Aerosil 300 ($\geq 99.8\%$, Evonik, $S_{\text{BET}} = 300 \pm 30 \text{ m}^2 \text{ g}^{-1}$, $V_{\text{pore}} = 0.56 \text{ ml g}^{-1}$), silicon carbide (≥ 98.8 , Alfa Aesar), sodium orthovanadate ($\geq 99.0\%$, Acros Organics), sodium oxalate ($\geq 99.5\%$, Sigma-Aldrich), and sodium nitrate ($\geq 99\%$, Acros Organics). $\beta\text{-NaVO}_3$ ¹ and $\alpha\text{-NaV}_2\text{O}_5$ ² were synthesized according to literature methods.

Catalysts. Aerosil 300 was dispersed in DI water and stirred until a homogenous slurry was achieved. The slurry was dried at $110 \text{ }^\circ\text{C}$ for two days and chunks of dry Aerosil 300 crushed and sieved to collect particles in the range of $150\text{-}300 (\pm 50) \mu\text{m}$. This fraction was calcined at $600 \text{ }^\circ\text{C}$ for 4 h to give a material with a surface area and a pore volume of $286 \text{ m}^2 \text{ g}^{-1}$ and 1.6 ml g^{-1} , respectively. $[\text{VO}_4]/\text{SiO}_2$ (**1**) was prepared by mixing aqueous NH_4VO_3 (0.297 M , 3.2 ml) with oxalic acid (3.2 ml , 0.55 M) followed by impregnated on SiO_2 (2 g) and calcination ($600 \text{ }^\circ\text{C}$, 4 h , $4 \text{ }^\circ\text{C min}^{-1}$). $\beta\text{-NaVO}_3/\mathbf{1}$ was prepared by dissolving $\beta\text{-NaVO}_3$ (0.070 g , 0.57 mmol) in 3.2 ml DI water and impregnating this solution on SiO_2 (2 g) followed by drying overnight at $100 \text{ }^\circ\text{C}$. This material ($\beta\text{-NaVO}_3/\text{SiO}_2$) was further impregnated with an aqueous solution of NH_4VO_3 (3.2 ml , 0.118 M) also containing 0.089 g of oxalic acid dihydrate, followed by drying overnight at $100 \text{ }^\circ\text{C}$ and calcination ($600 \text{ }^\circ\text{C}$, 4 h , $4 \text{ }^\circ\text{C min}^{-1}$) under static air in a muffle furnace. The same procedure was used to prepare $\alpha\text{-NaVO}_3/\mathbf{1}$ except that $\alpha\text{-NaVO}_3$ was used instead of $\beta\text{-NaVO}_3$. $\text{Na}_{1+x}\text{V}_3\text{O}_8/\text{SiO}_2$ was prepared by impregnating SiO_2 (2 g) with $\text{Na}_{1+x}\text{V}_3\text{O}_8$ (3.2 ml , 0.1 M) dispersed in water at $70 \text{ }^\circ\text{C}$, drying overnight at $100 \text{ }^\circ\text{C}$ and calcination ($600 \text{ }^\circ\text{C}$, 4 h , $4 \text{ }^\circ\text{C min}^{-1}$).

Characterization. Brunauer–Emmett–Teller (BET)³ and Barrett–Joyner–Halenda (BJH)⁴ models were used to calculate the surface area and pore volume, respectively. Samples were outgassed at $300 \text{ }^\circ\text{C}$ for 3 h prior to nitrogen physisorption at $-196 \text{ }^\circ\text{C}$ using a NOVA4000e (Quantachrome) instrument. X-ray diffractograms were collected with an PANalytical Empyrean X-ray powder diffractometer (45 kV and 40 mA) using Cu K_α as an X-ray source. The XRD instrument is equipped with an X'Celerator Scientific ultrafast line detector and Bragg–Brentano HD incident beam optics. All scans were performed in the 2θ range of $5\text{-}100$ with a step size of 0.017 (0.65 s acquisition time per step). ^{51}V and ^{23}Na solid state nuclear magnetic resonance (ssNMR) spectra were collected using an Avance NMR spectrometer (Bruker) operating at a ^1H Larmor frequency of 400 MHz . The magic angle spinning rate was between $15\text{-}18 \text{ kHz}$ for all samples using a double resonance 3.2 mm probe and N_2 as bearing, drive, and VT flow gas. The probe was tuned to 105.246 and 105.842 MHz for V and Na nuclei, respectively. The ^{13}C signal of adamantane was used as an external secondary reference to calibrate the ppm scale of the spectra. All rotors were filled in a dry glovebox under N_2 atmosphere (H_2O and $\text{O}_2 < 0.5 \text{ ppm}$) and transferred under N_2 environment to the spectrometer except for the unsupported reference materials. A DXR 2 Raman microscope (Thermo Fischer) equipped with a high-temperature Linkam CCR1000 cell was used for ex and in situ measurements. A 455 nm excitation laser with a full range grating ($100\text{-}3500 \text{ cm}^{-1}$, $1200 \text{ lines mm}^{-1}$) was used to collect all spectra at room temperature. For dehydration, samples were treated inside an in situ cell at $500 \text{ }^\circ\text{C}$ under dry air and cooled down to room temperature prior to spectra collection. Each spectrum reported here is an average of 10 spectra collected from different positions on the sample to ensure reproducibility and homogeneity. X-ray absorption spectroscopy (XAS) was collected at the V K-edge at the SuperXAS beamline of the Swiss Light Source (SLS) of the Paul Scherer Institute (PSI). XAS spectra were collected under transmission mode for bulk materials and under fluorescence mode for the supported materials, respectively. Supported samples were dehydrated at $500 \text{ }^\circ\text{C}$ under flowing air (30 ml min^{-1}) for 1 h in a quartz reactor and cooled down under air to room temperature. Dehydrated samples were purged under N_2 for 30 min and transferred to a glovebox without exposure to atmosphere. Dehydrated samples were filled in quartz capillaries (1 mm ID) and sealed with paraffin and vacuum grease for fluorescence measurements. The Demeter software package⁵ was used to process the X-ray absorption near the edge (XANES) and fit the extended X-ray absorption fine structure (EXAFS) data. Temperature programmed reduction (TPR) profiles of the studied materials were collected using a commercial BELCAT-M machine (BEL JAPAN, INC). 50 mg of sample was fixed between two quartz wool plunges in a U-shape quartz tube and degassed/dehydrated for 1 h at $300 \text{ }^\circ\text{C}$ under Ar (50 ml min^{-1}). After cooling down to $100 \text{ }^\circ\text{C}$, the gas flow was changed to $5\% \text{ H}_2$ in Ar (50 ml min^{-1}) and the temperature was increased to $750 \text{ }^\circ\text{C}$ with a ramp rate of $10 \text{ }^\circ\text{C min}^{-1}$ while recording TCD data. Differential scanning calorimetry (DSC) analysis was carried out using a Mettler Toledo TGA/DSC 3+ instrument equipped with Bronkhorst mass flow controllers (MFC) to adjust gas flows. A platinum crucible was used. Scanning electron microscopy and energy dispersive X-ray mapping (STEM-EDX) were acquired using a TEM (FEI Talos F200X) equipped with a high-brightness field-emission gun, a high-angle annular dark field (HAADF) detector, and a large collection-angle EDX detector. The operation voltage of the instrument was set to 200 kV in scanning transmission electron microscopic (STEM) mode. Inductively coupled plasma-optical emission spectroscopy (ICP-OES) was carried out on an Agilent 5100 VDV. For calibration, multi-element standard was utilized. To lessen matrix effects, the matrix acid for all blanks, standards and samples were matched. Each sample was diluted such that the elemental concentrations were in the linear range of the standard and detector combination. Samples were prepared by digesting $3\text{-}4 \text{ mg}$ of a sample with 5 ml of aqua regia ($3:1 \text{ HCl:HNO}_3$) in a microwave digestion system (Multiwave GO) at $175 \text{ }^\circ\text{C}$ for 30 min. The resulting solutions were subsequently diluted to 25 ml with deionized water. To avoid contamination, trace-grade acids (HCl and HNO_3) were used.

Catalytic tests. Catalytic tests were performed in a 10 mm internal diameter (ID) quartz reactor in a PID Microactivity-Effi integrated reactor using 100 mg of catalyst ($150\text{-}300 \mu\text{m}$) mixed with 200 mg of SiC (46 grit particles) to avoid hot spot formation. The oxidative dehydrogenation of propane (ODP) was carried out using a total flow of 21 ml min^{-1} of a mixture of propane and air ($2 : 5$) at $450 \text{ }^\circ\text{C}$. Off-gases were analyzed by a Clarus 580 GC equipped with a methanizer. All carbon based products including CO_x were separated by a HP Plot Q Restek column and analyzed by a flame ionization detector (FID). H_2 , N_2 , and O_2 were separated by a ShinCarbon ST 80/100 Restek column and analyzed by a thermal conductivity detector (TCD). Catalysts were heated under air up to $450 \text{ }^\circ\text{C}$ ($10 \text{ }^\circ\text{C min}^{-1}$) and were kept at this temperature for 60 min to stabilize the temperature before the reactants were introduced to the reactor. The first data point was collected after 10 min of reaction and continued for 240 min every 20 min. The carbon balance of each

data point closes within 3 %. Selectivity and productivity vs. conversion plots have been obtained by varying the total flow of the reactants between 15.8 and 42 ml min⁻¹ while keeping the same propane-to-air ratio of 2 to 5. For a typical experiment, 100 mg of the catalyst was heated up to 450 °C under a synthetic airflow of 21 ml min⁻¹ and kept at this temperature for 1 h before the reactants are introduced. Starting from the lowest contact time (WHSV = 13.6 h⁻¹), two GC data points were collected for each WHSV (approximately 30 min of TOS). This was followed by increasing the contact time, while keeping the propane to air ratio constant, to obtain additional data for WHSV = 10.2, 6.8, and 5.1 h⁻¹. As the promoted catalysts lose their activity with time on stream, we have used fresh catalysts for different temperatures while the same catalyst was used for measurements at a constant temperature.

Equations

$$\text{Surface density (V}_{\text{atoms}} \text{ nm}^{-2}) = \frac{M \times \text{Avogadro number} \times 10^{-18}}{\text{SA (m}^2 \text{ g}^{-1}) \times \text{grams of support}},$$

M is the moles of V in the catalyst, SA is the surface area of Aerosil

$$\text{Selectivity of carbon product } i = \frac{y_i F_{\text{C}_3\text{H}_6} \text{ (ml min}^{-1}\text{)}}{\sum y_i F_{\text{carbon product}} \text{ (ml min}^{-1}\text{)}}, \text{ F is the flow rate}$$

, y_i is the number of carbons in product i

$$\text{Specific activity (C}_3\text{H}_6) = \frac{F_{\text{C}_3\text{H}_6} \text{ (ml s}^{-1}\text{)}}{M \times 24450 \text{ (ml mol}^{-1}\text{)}} \text{ (where } 24450 \text{ ml mol}^{-1} \text{ is the molar volume of a gas at STP)}$$

$$\text{WHSV} = \frac{F_{\text{C}_3\text{H}_8} \text{ (ml h}^{-1}\text{)} \times M_w \text{ (g mol}^{-1}\text{)}}{24450 \text{ (ml mol}^{-1}\text{)} \times \text{grams of the catalyst}}, M_w \text{ is the molecular weight of propane}$$

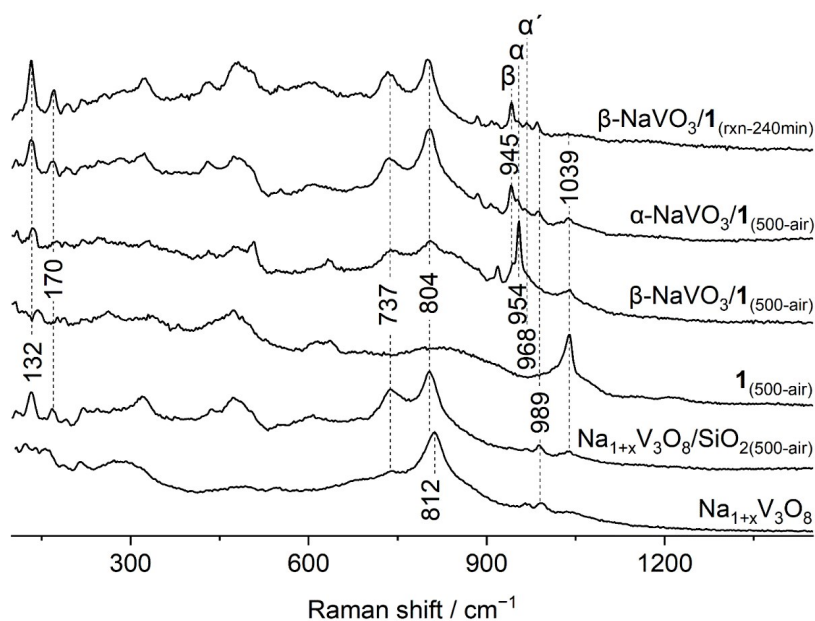


Figure S1. Raman spectra of the studied materials in the range 100–1450 cm^{-1} .

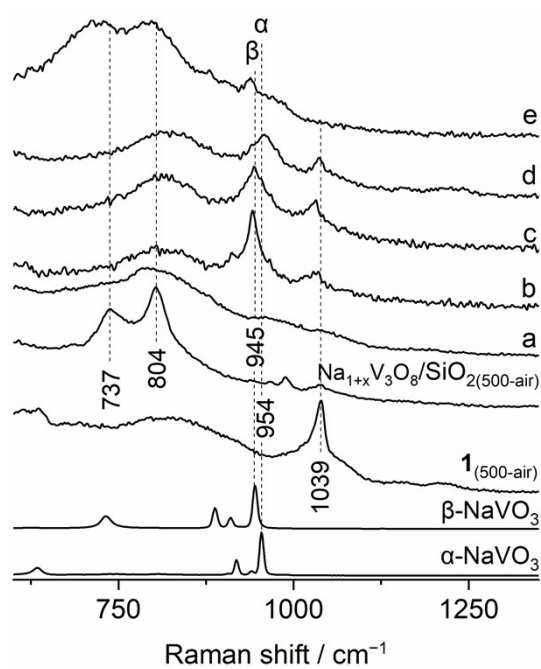


Figure S2. Raman spectra of $\alpha\text{-NaVO}_3/1$ during in situ calcination (Linkam CCR1000 cell).

Calcination was carried out using $4\text{ }^\circ\text{C min}^{-1}$ temperature ramp rate up to $600\text{ }^\circ\text{C}$ for 4 h under 30 ml min^{-1} air. The spectra correspond to the as-prepared $\alpha\text{-NaVO}_3/1$ at room temperature (a), at ca. $600\text{ }^\circ\text{C}$ (b, c) and again at room temperature after the calcination (d, e). Different areas of the specimen were surveyed and representative spectra are presented.

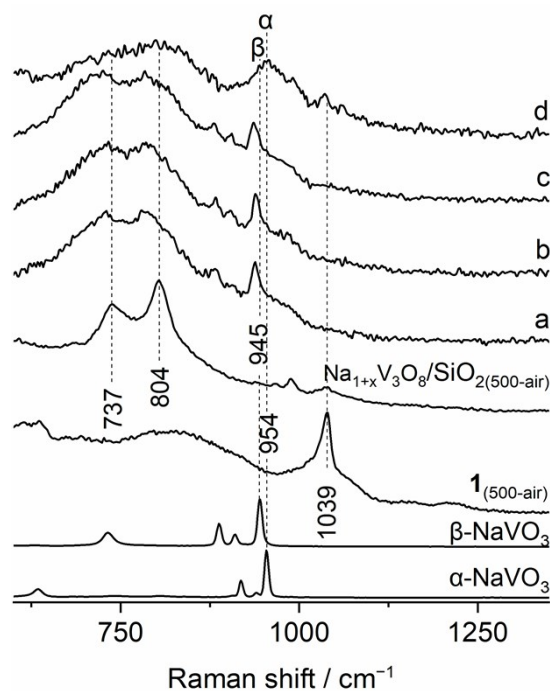


Figure S3. Room temperature Raman spectra of different areas of calcined α - $\text{NaVO}_3/1$ (traces a-d) after exposure to air.

Calcination was carried out in a muffle furnace at 600 °C for 4 h using 4 °C min⁻¹ temperature ramp under static air. The calcined material was then re-hydroxylated by opening to ambient air, which accounts for the red shift in the band positions compared to dehydroxylated materials presented in Figure 1 of the main text.

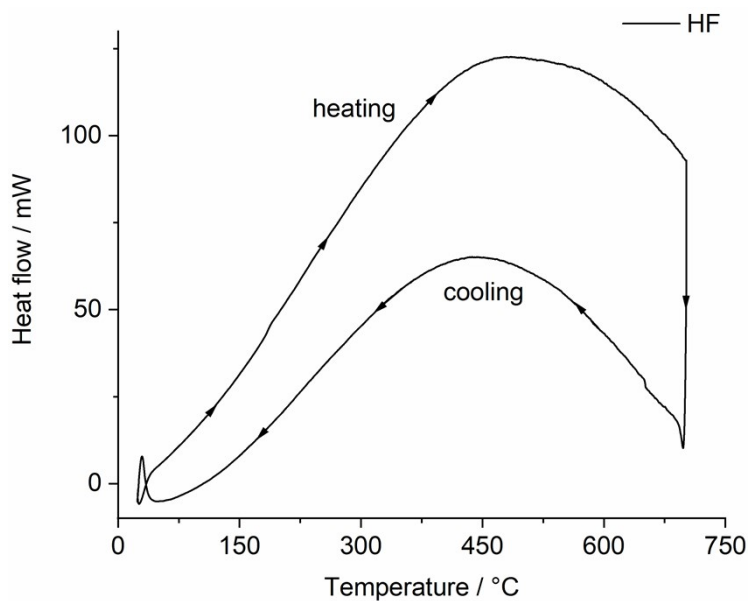


Figure S4. DSC measurement of α - $\text{NaVO}_3/1$ calcination.

Calcination was carried out under 30 ml min⁻¹ airflow with a 4 °C min⁻¹ temperature ramp rate up to 700 °C for 4h.

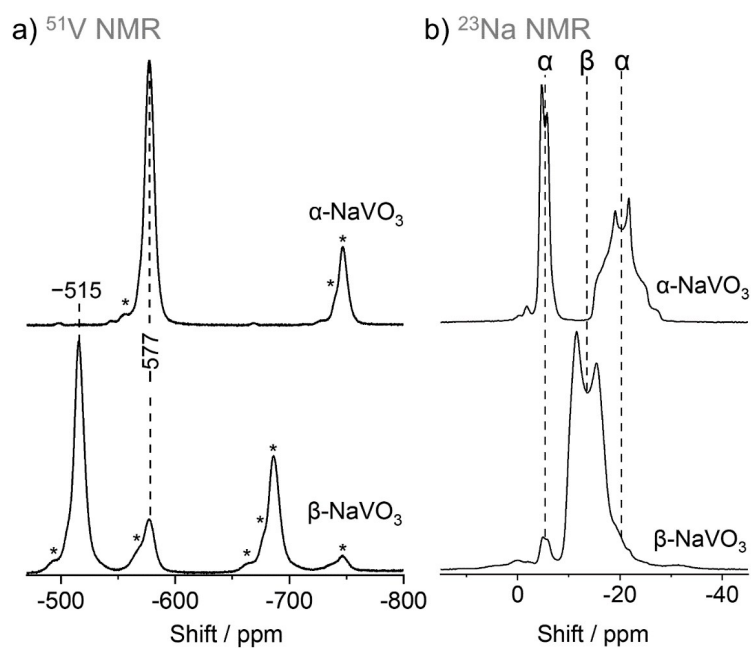


Figure S5. (a) ^{51}V , and (b) ^{23}Na MAS NMR data for as synthesized $\beta\text{-NaVO}_3$ and $\alpha\text{-NaVO}_3$.

Spinning side bands in the NMR spectra are marked by asterisks (spinning rates of 15-18 kHz were used). $\beta\text{-NaVO}_3$ contains minor amounts of $\alpha\text{-NaVO}_3$.

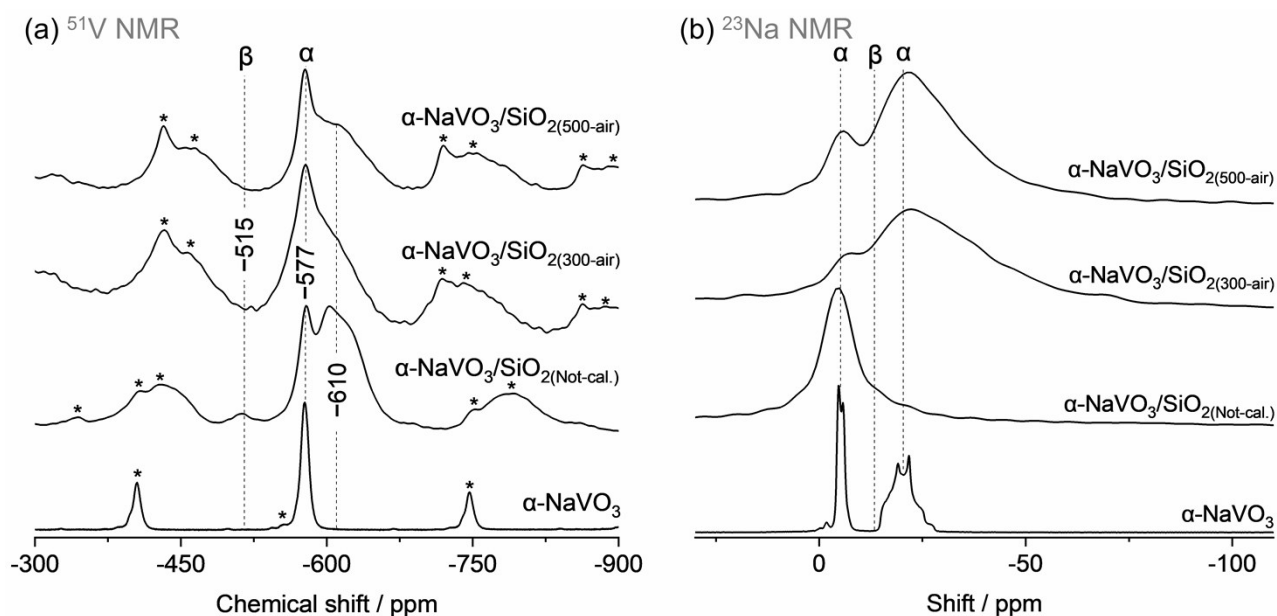


Figure S6. (a) ^{51}V and (b) ^{23}Na MAS NMR of $\alpha\text{-NaVO}_3/\text{SiO}_2$ (catalyst made from $\beta\text{-NaVO}_3$ precursor).

Spinning rates of 15-18 kHz, side bands are marked by asterisks. Not-cal. subscript stands for Not calcined material after drying at 100 °C.

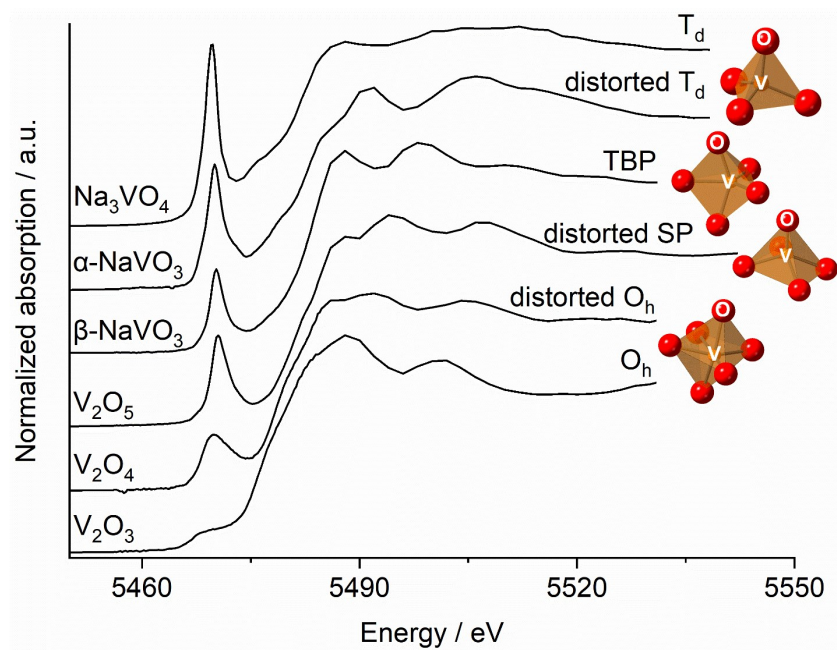


Figure S7. V K-edge XANES spectra of the reference compounds selected to show the dependence of the pre-edge peak height on the ligand geometry of vanadium.

T_d , TBP, SP, and O_h stands for tetrahedral, trigonal bipyramidal, square pyramidal, and octahedral, respectively,

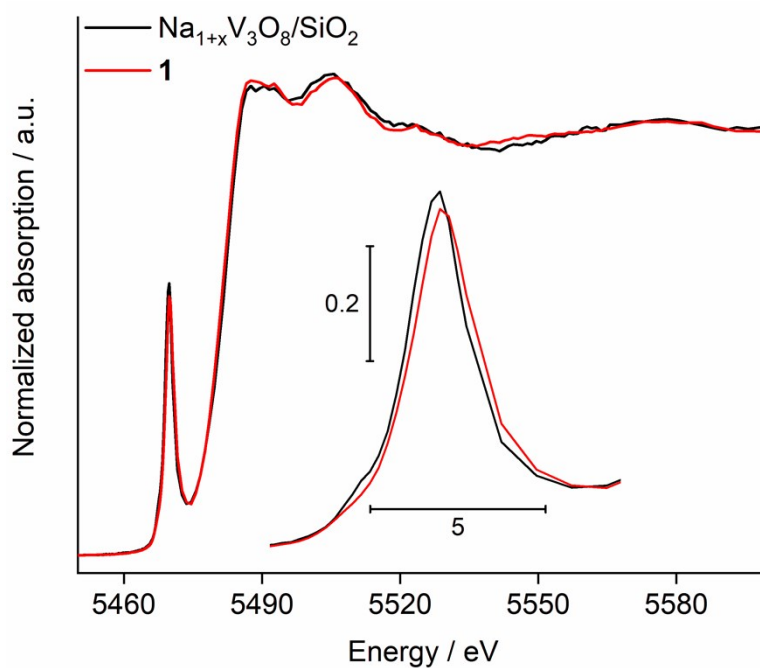


Figure S8. XANES spectra of $Na_{1+x}V_3O_8/SiO_2$ vs **1** (hydrated).

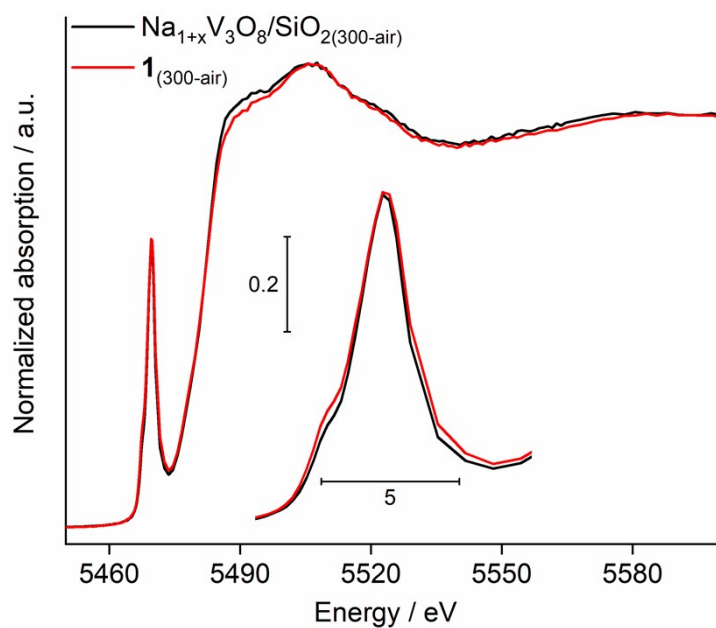


Figure S9. XANES spectra of $\text{Na}_{1+x}\text{V}_3\text{O}_8/\text{SiO}_2(\text{air-300})$ and $\mathbf{1}_{(\text{air-300})}$ (dehydrated).

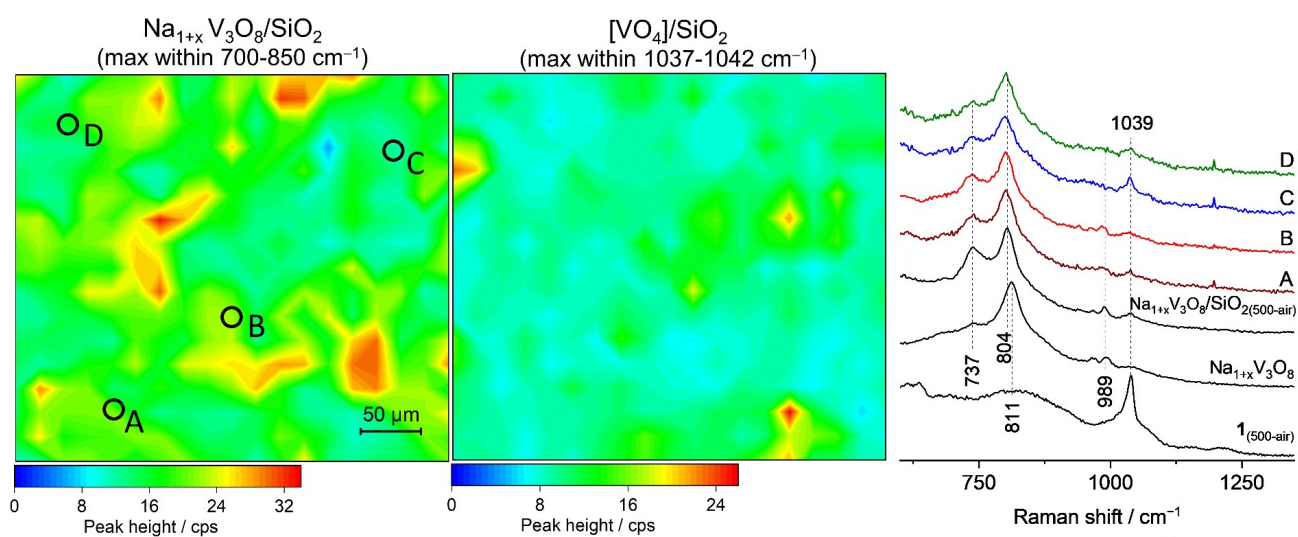


Figure S10. Raman mapping of $\text{Na}_{1+x}\text{V}_3\text{O}_8/\text{SiO}_2(\text{air-500})$.

Raman mapping performed with 323 points (19×17 : $x \times y$) separated by $20 \mu\text{m}$ (the laser spot size was ca. $1.6 \mu\text{m}$) using intensities of the characteristic Raman peaks at 804 cm^{-1} and $1039 (\pm 2 \text{ cm}^{-1})$ to map $\text{Na}_{1+x}\text{V}_3\text{O}_8/\text{SiO}_2$ and $[\text{VO}_4]/\text{SiO}_2$, respectively. Raman spectra of selected points are shown in the right panel.

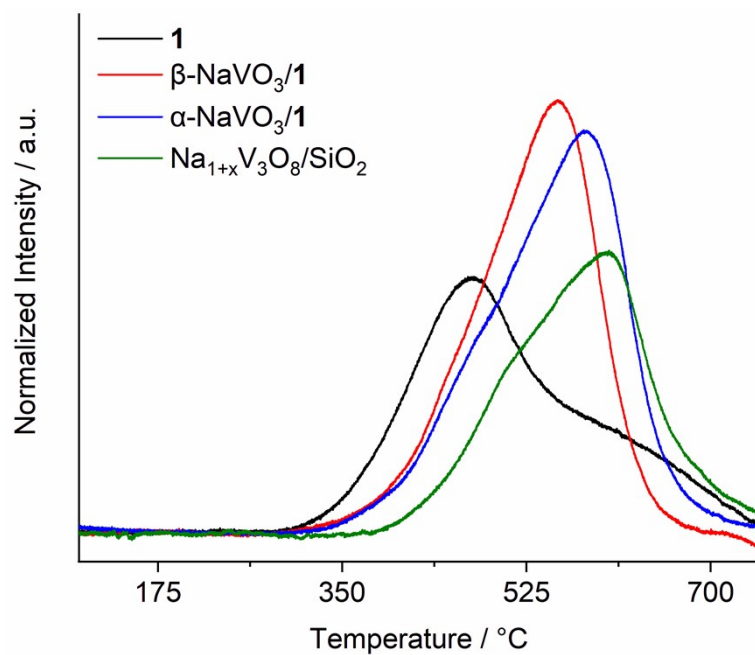


Figure S11. H₂ temperature-programmed reduction (TPR) profile of the studied catalysts.

TPR profiles of **1** has been reported by us previously and are given here comparison.⁶

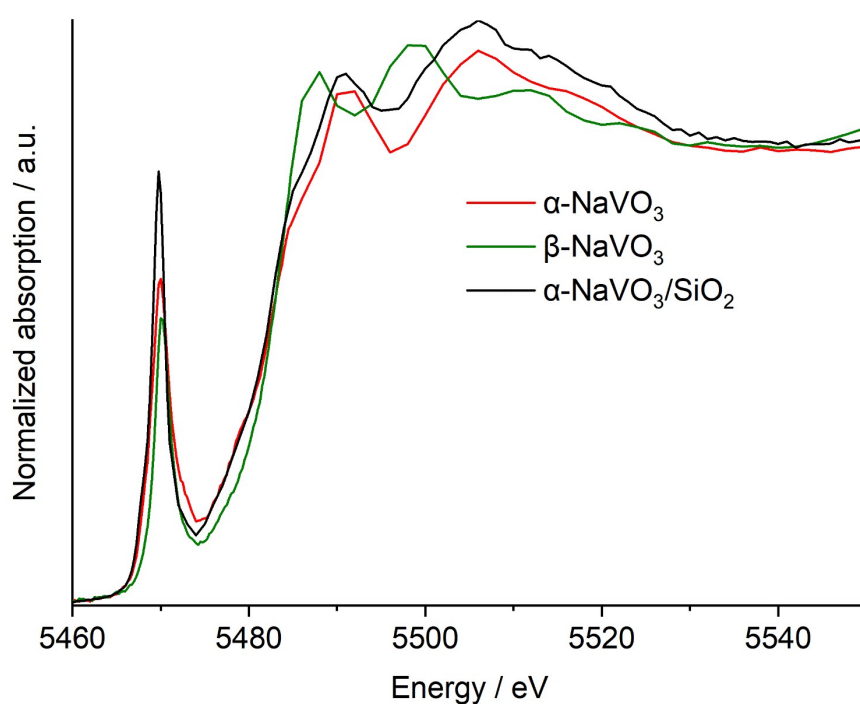


Figure S12. V K-edge XANES spectra of α -NaVO₃/SiO₂ (synthesized from β -NaVO₃), β -NaVO₃ and α -NaVO₃.

The transformation of β -NaVO₃ to α -NaVO₃ after supporting it on silica and calcination at 600 °C can be seen from the XANES spectrum.

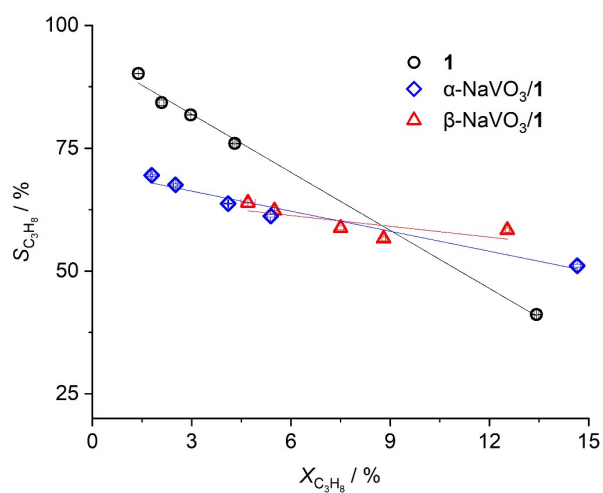


Figure S13. Selectivity vs. conversion plot for studied catalysts.

The WHSV was varied between 5.1-13.6 h^{-1} by changing the total flow rate (15.8 - 42 $ml\ min^{-1}$) and using 100 mg of catalysts, for conversions of propane < 10%. However, for higher conversions (>12%), lower WHSV of 1.7-3.4 h^{-1} were achieved when using a total flow of 10.5 $ml\ min^{-1}$ and 100-200 mg of fresh catalysts.

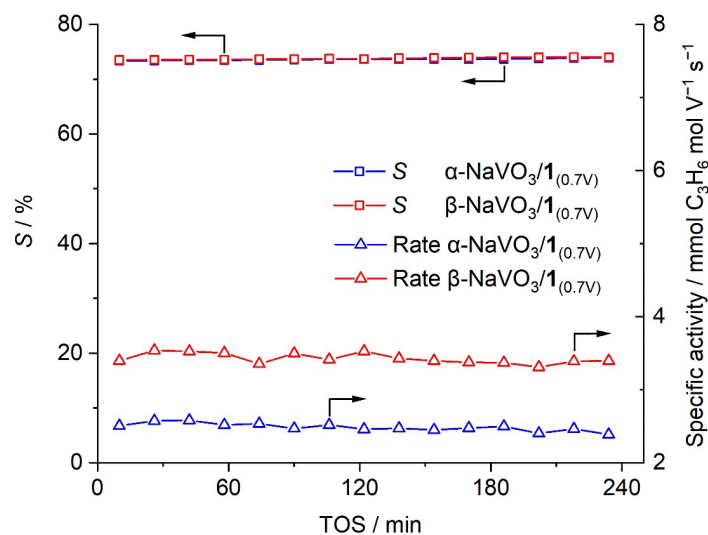


Figure S14. ODP propene selectivity and specific activity with TOS for β - and α - $NaVO_3/1_{(0.7)}$

(C_3H_8 : air = 2 : 5, total flow of 21 $ml\ min^{-1}$, 450 $^{\circ}C$)

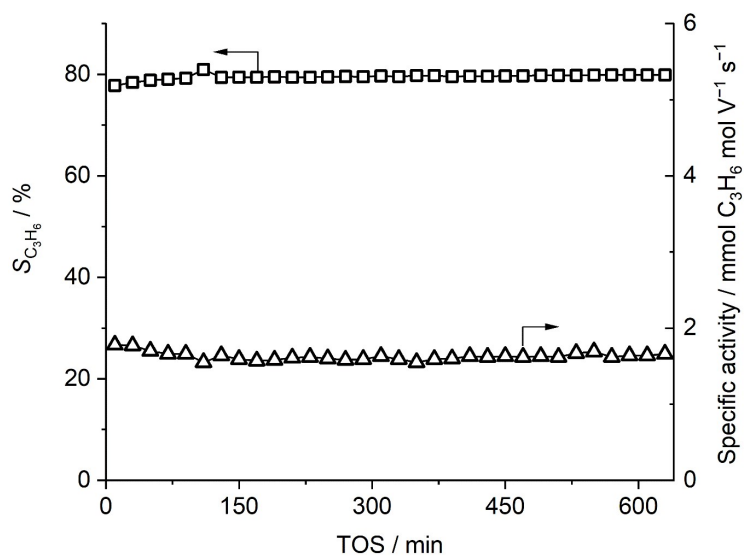


Figure S15. Propene selectivity and production rate vs TOS for $\text{Na}_{1+x}\text{V}_3\text{O}_8/\text{SiO}_2$.

The sample was heated under synthetic air and kept at 450 °C for 1 h prior to reaction start. C_3H_8 : air = 2 : 5, 21 ml min⁻¹ total flow, 450 °C.

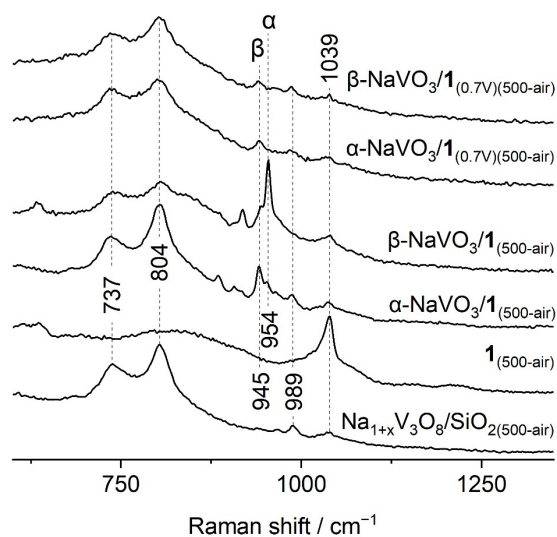


Figure S16. Raman spectra of $\alpha\text{-NaVO}_3/1_{(0.7)}$ and $\beta\text{-NaVO}_3/1_{(0.7)}$ compared to the other materials.

Samples are dehydrated at 500 °C under 30 ml min⁻¹ synthetic air.

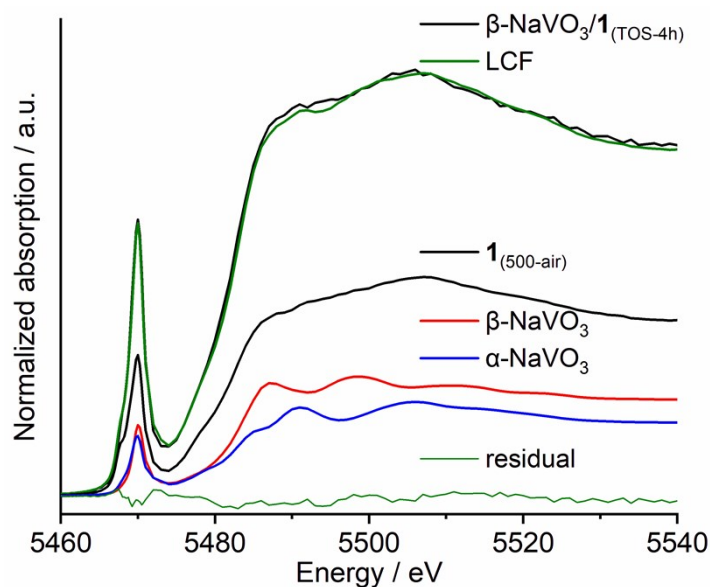


Figure S17. Linear combination fitting (LCF) of the V K-edge XANES of β - $\text{NaVO}_3/1$ after 4h of reaction under ODP conditions.

C_3H_8 : air = 2 : 5, total flow of 21 ml min^{-1} , $450 \text{ }^\circ\text{C}$, heated up under air. Sample was handled under inert atmosphere.

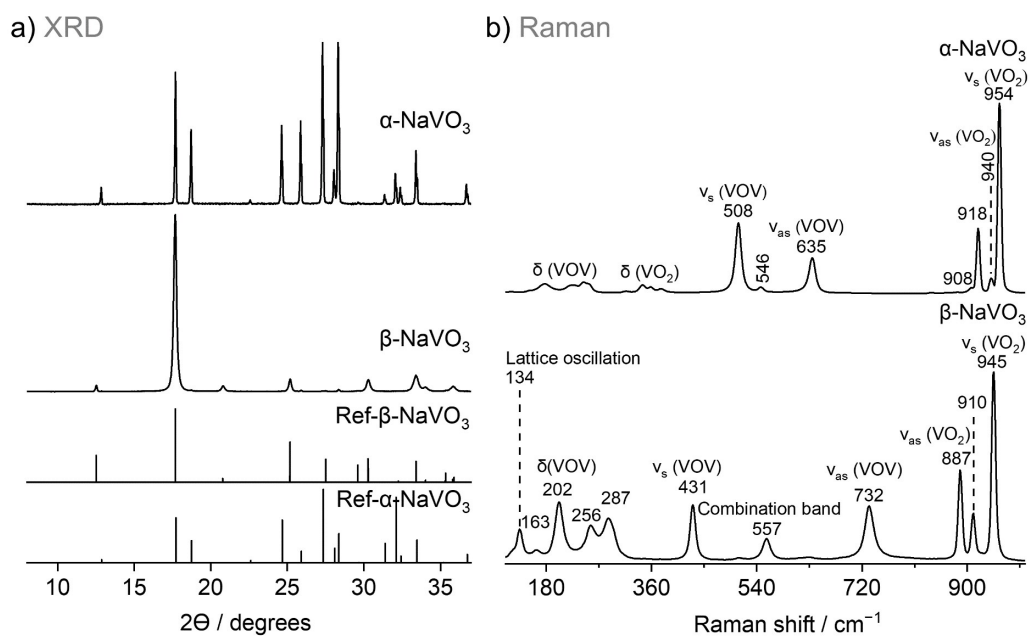


Figure S18. a) XRD and b) Raman data for as synthesized β - NaVO_3 and α - NaVO_3 .

Raman assignments are given according to the literature.¹ ν_s , ν_{as} , and δ are symmetric, asymmetric stretching, and bending vibrations modes, respectively. β - NaVO_3 contains minor amounts of α - NaVO_3 .

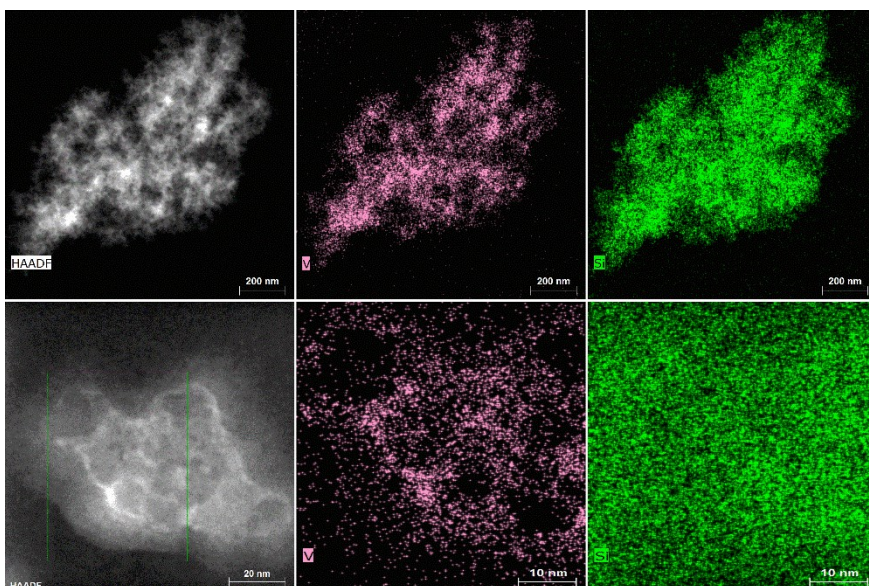


Figure S19. High-angle annular dark field (HAADF) scanning transmission electron microscopy (STEM) and energy dispersive X-ray (EDX) mapping of **1**.

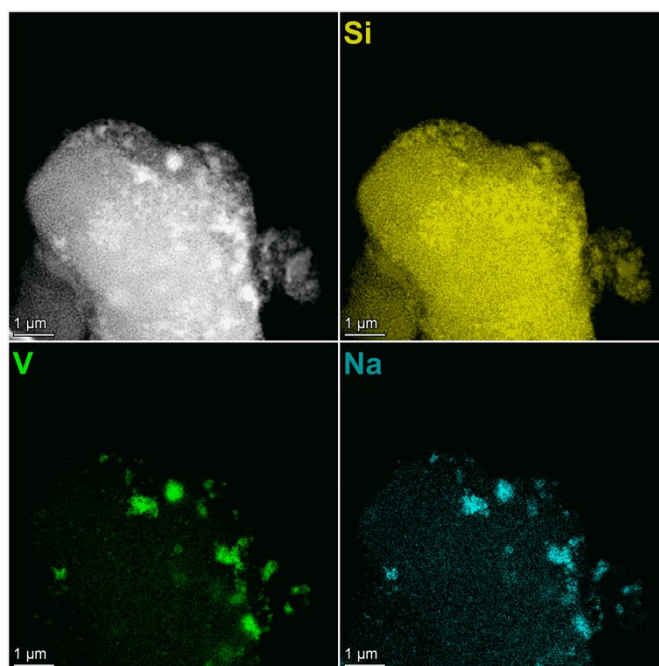


Figure S20. High-angle annular dark field (HAADF) scanning transmission electron microscopy (STEM) and energy dispersive X-ray (EDX) mapping of α -NaVO₃/**1**.

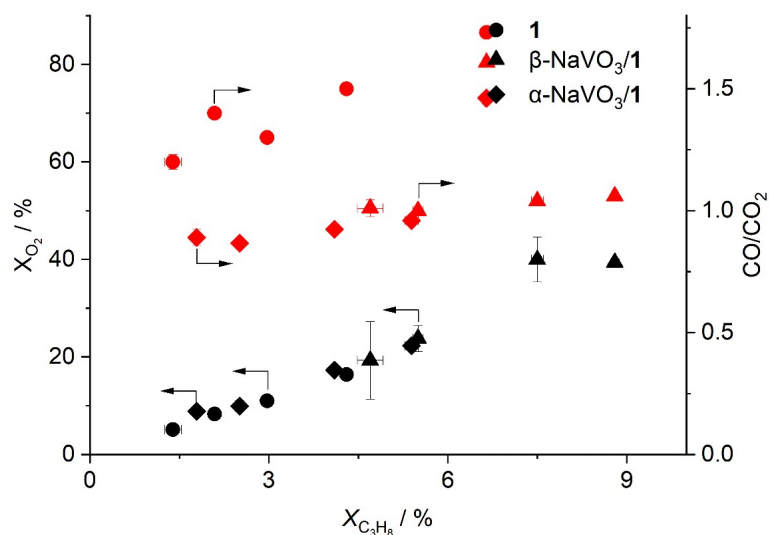


Figure S21. O_2 conversions (X_{O_2}) and CO/CO_2 molar ratios vs propane conversions ($X_{C_3H_8}$) for the studied catalysts.

The WHSV was varied between $5.1\text{--}13.6\text{ h}^{-1}$ by varying the total flow rate ($15.8\text{--}42\text{ ml min}^{-1}$) of the feed at $450\text{ }^\circ\text{C}$. Partial pressures of propane and oxygen were always 0.3 and 0.15 bar (balance N_2), respectively. X_{O_2} and CO/CO_2 ratio of **1** have been reported previously by us,⁶ and are given here for the sake of comparison.

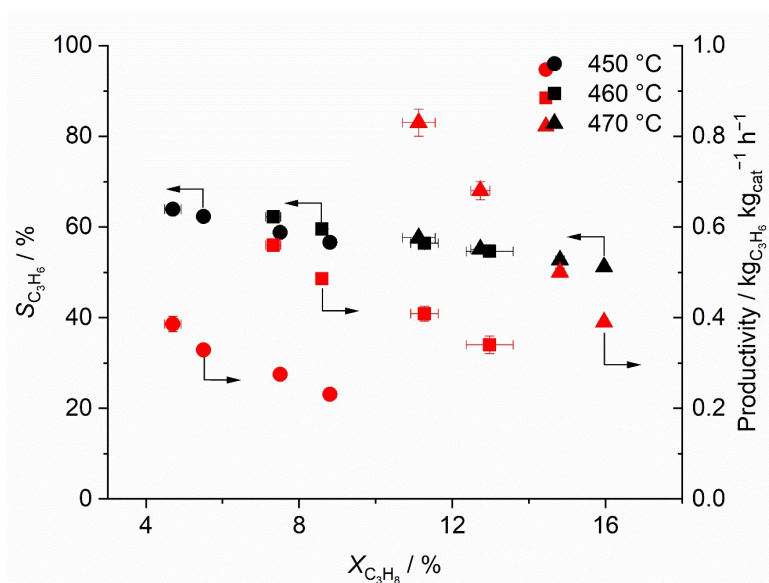


Figure S22. Propene selectivity ($S_{C_3H_6}$) and productivity vs propane conversion ($X_{C_3H_8}$) at different temperatures for air treated (1 h) $\beta\text{-NaVO}_3/1$ catalyst.

The WHSV was varied between $5.1\text{--}13.6\text{ h}^{-1}$ by varying the total flow rate ($15.8\text{--}42\text{ ml min}^{-1}$) of the feed. Partial pressures of C_3H_8 and O_2 were always 0.3 and 0.15 bar (balance N_2), respectively.

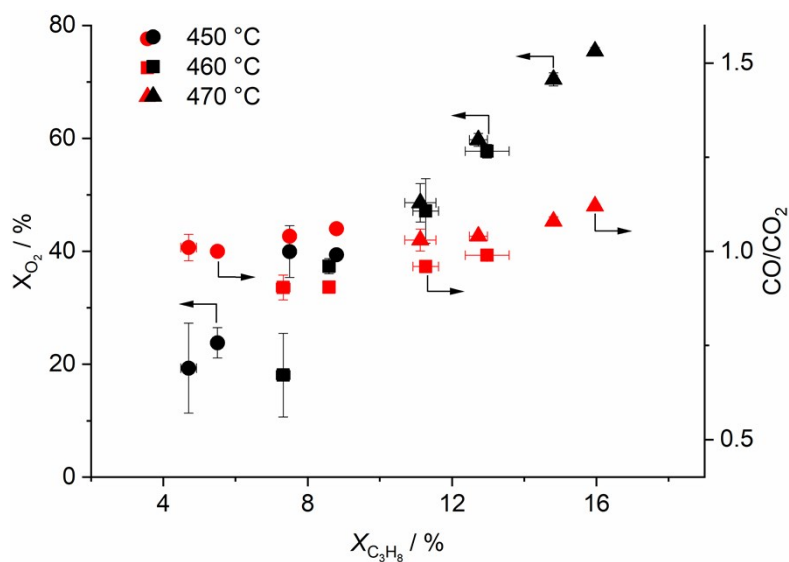


Figure S23. O₂ conversions (X_{O_2}) and CO/CO₂ molar ratios vs propane conversions ($X_{C_3H_8}$) at different temperatures for β -NaVO₃/1.

For each temperature a new sample was used and the catalyst was heated up under air and kept at the designated temperature for 1 h prior to the reaction start. The WHSV was varied between 5.1-13.6 h⁻¹ by varying the total flow rate (15.8-42 ml min⁻¹) of the feed at different temperatures. Partial pressures of propane and oxygen were always 0.3 and 0.15 bar (balance N₂), respectively.

Table S1. N₂ physisorption and ICP data of studied catalysts.

Entry	Catalyst	Nominal surface density (V nm ⁻²)	Nominal Na/V molar ratio	BET surface area (m ² g ⁻¹)	Vanadium wt% by ICP	Na/V molar ratio by ICP	Surface density in calcined catalysts (V nm ⁻²)
1	[VO ₄]/SiO ₂ (1)	1	n.a.	217	2.1	n.a.	1.1
2	Na _{1+x} V ₃ O ₈ /SiO ₂	1	0.33	215	2.1	-	1.1
3	α -NaVO ₃ /1	1	0.60	145	1.9	0.63	1.6
4	β -NaVO ₃ /1	1	0.60	120	2.0	0.62	2.0
5	α -NaVO ₃ /1 _(0.7V)	0.7	0.30	156	1.6	0.35	1.2
6	β -NaVO ₃ /1 _(0.7V)	0.7	0.30	184	1.5	0.32	1.0

References

1. Seetharaman, S.; Bhat, H. L.; Narayanan, P. S., Raman spectroscopic studies on sodium metavanadate. *J. Raman Spectrosc.* **1983**, *14*, 401-405.
2. Liu, P.; Zhou, D.; Zhu, K.; Wu, Q.; Wang, Y.; Tai, G.; Zhang, W.; Gu, Q., Bundle-like α' - NaV_2O_5 mesocrystals: from synthesis, growth mechanism to analysis of Na-ion intercalation/deintercalation abilities. *Nanoscale* **2016**, *8*, 1975-1985.
3. Brunauer, S.; Emmett, P. H.; Teller, E., Adsorption of Gases in Multimolecular Layers. *J. Am. Chem. Soc.* **1938**, *60*, 309-319.
4. Barrett, E. P.; Joyner, L. G.; Halenda, P. P., The Determination of Pore Volume and Area Distributions in Porous Substances. I. Computations from Nitrogen Isotherms. *J. Am. Chem. Soc.* **1951**, *73*, 373-380.
5. Ravel, B.; Newville, M., ATHENA, ARTEMIS, HEPHAESTUS: data analysis for X-ray absorption spectroscopy using IFEFFIT. *J. Synchrotron Rad.* **2005**, *12*, 537-541.
6. Nadjafi, M.; Abdala, P. M.; Verel, R.; Hosseini, D.; Safonova, O. V.; Fedorov, A.; Müller, C. R., Reducibility and Dispersion Influence the Activity in Silica-Supported Vanadium-Based Catalysts for the Oxidative Dehydrogenation of Propane: The Case of Sodium Decavanadate. *ACS Catal.* **2020**, *10*, 2314-2321.